Biocompatible a-SiC:H-Based Bistable MEMS Membranes With Piezoelectric Switching Capability in Fluids

Philipp Moll, Georg Pfusterschmied, Michael Schneider, Manuel Dorfmeister, Sebastian Knafl, Heinz D. Wanzenboeck, and Ulrich Schmid

***Abstract*— In this paper, we demonstrate biocompatible micromachined buckled membranes for the operation in liquids. The membranes feature diameters between 600 and 800 μm as well as integrated piezoelectric thin film actuators, thus enabling switching between the bistable states. The membrane material is known to be not biocompatible, hence a hydrogenated amorphous silicon carbide (a-SiC:H) layer is deposited on the surface. For demonstration purposes, a 70 nm ±3 nm thin a-SiC:H coating with a specific silicon to carbon ratio was chosen, with a negligible impact on the overall switching performance of the bistable membranes. Furthermore, a relation between the membrane center velocity at the first characteristic resonance frequency and the switching ability of a membrane in different viscous fluids is shown. Based on a small signal analysis the switching behavior can be predicted. The membranes were successfully switched in liquids with a dynamic viscosity up to 286 mPa·s. The biocompatibility of the membranes was examined by growing Caco-2 cells, a human carcinoma cell line, on a-SiC:H thin films, featuring different carbon contents and organic surface treatments. The proliferation and adhesion of the cells on the substrates are examined in an empirical cell growth and removal study. Only a-SiC:H surfaces pre-treated with an O2-plasma and coated with Collagen Type I indicated to provide an environment of improved cell adhesiveness compared to other surface treatments. The biological investigations resulted in good cell proliferation, that also depends on the altered hydrophilicity of the surface, as well as on the carbon content of the a-SiC:H thin films. This study reveals that a broad range of biocompatible a-SiC:H surfaces can be prepared, whereby the cell growth can be tailored in terms of proliferation and adhesion for different biomedical application scenarios. Finally, this paper reports on the mechanical features of bistable, buckled membranes and their suitability as a growth substrate for human cell cultures, due to the good biocompatibility of a-SiC:H thin films. We therefore suggest that it will be feasible to grow cells on bistable MEMS membranes, enabling cell experiments in liquid medical environments, with both mechanically excitable and biocompatible surfaces. [2022-0006]**

***Index Terms*— Aluminum nitride, amorphous semiconductors, bi-stable membrane, bio-inspired engineering, cells (biology), biological interactions, biomedical electronics, MEMS, microactuators, microelectromechanical systems, piezoelectric transducers, silicon carbide.**

I. Introduction

IN THE last two decades, biomedical microelectromechanical systems (Bio-MEMS) have revolutionized the way medicine is practiced and delivered. Bio-MEMS have tremendously contributed to the increase of the quality of life for human patients suffering from diseases [1], [2]. In the course of this success story a fully integrated battery-free MEMS pressure sensor for the detection of arterial stenosis and stroke prevention has already been presented in 2006 by DeHennis and Wise [3]. Another prominent Bio-MEMS example are controlled-release systems for drug-delivery applications. They first appeared in the 1960s and 1970s and were miniaturized and drastically improved at the turn of the millennium [4]–[6], enabling vital precise integrated insulin delivery [7]. Giving only these selected examples, the importance of MEMS in the field of medicine cannot be denied. However, the direct contact of MEMS devices with living cells is a challenge, especially for in vivo sensor systems. This is because common MEMS devices are often fabricated with standard MEMS materials such as nickel [8], [9], chromium [10], [11] or aluminum nitride [12]–[18] as one of the most important piezoelectric materials for MEMS, making them hazardous for the human body [19], [20]. Moreover, gallium arsenide or tungsten are even rated with 3 and 2 in the Hazardous Materials Identification System (HMIS), impeding their implementation for medical applications.

Yet, a biocompatible coating on a MEMS device with adjustable mechanical properties would open new application scenarios in the biomedical field. Since crystalline silicon carbide is already well-known as biocompatible material, but expensive and difficult to integrate into an existing silicon MEMS device fabrication process [21], hydrogenated amorphous silicon carbide (a-SiC:H) is regarded as promising material system. As a-SiC:H can be deposited as thin film on MEMS devices, it could be the ideal biocompatible surface coating, making a standard MEMS device to a truly biocompatible Bio-MEMS device.

In previous works we have investigated the switching behavior of piezoelectric micromachined buckled membranes in air [22], [23] and liquids [24]. Such membranes consist of

Manuscript received January 13, 2022; revised March 15, 2022; accepted March 17, 2022. Date of publication April 7, 2022; date of current version June 2, 2022. Subject Editor E. Meng. *(Corresponding author: Philipp Moll.)*

Philipp Moll, Georg Pfusterschmied, Michael Schneider, Manuel Dorfmeister, and Ulrich Schmid are with the Institute of Sensor and Actuator Systems, Vienna University of Technology, 1040 Vienna, Austria (e-mail: philipp.moll@tuwien.ac.at).

Sebastian Knafl and Heinz D. Wanzenboeck are with the Institute of Solid State Electronics, Vienna University of Technology, 1040 Vienna, Austria.

Color versions of one or more figures in this article are available at https://doi.org/10.1109/JMEMS.2022.3163477.

Digital Object Identifier 10.1109/JMEMS.2022.3163477

chromium as well as aluminum nitride, which classify them as non-biocompatible. In this paper we utilize our membranes to present a biocompatible coating for MEMS devices. Nevertheless, not just the biocompatibility, but also the mechanical properties of the coating are important. The challenge is to make a MEMS device biocompatible without compromising its mechanical performance/function. Specifically, for buckled membranes the stress window to show buckling and furthermore to exhibit a bistable behavior is very narrow. Leaving this optimal stress range leads to a significant rise of the required actuator energy, which should be kept as low as possible [22]. An advantageous characteristic of a-SiC:H is that stress and layer thickness can be controlled precisely by adjusting the gas flow [25]. Furthermore, a-SiC:H can be deposited at room temperature, which opens the opportunity to coat MEMS devices with temperature sensitive materials.

The controllable oscillating and switching behavior in combination with biocompatible properties would have a tremendous impact on the field of cell investigation. The substrate can be used to mechanically stimulate the cells, mimicking the biomechanical situation in a living body due to pulsating blood flow or due to breathing.

It is well known that biomechanical factors have a lasting influence in cell proliferation, differentiation and in their metabolism [26], [27]. To specifically tailor the capability of a MEMS device for high or low cell adhesion is crucial for many applications. On one hand, selected microfluidic cell applications such as valves for blood flow simulation require very low cell attachment on the actual membrane working as microfluidic valves. On the other hand, cell cultures growing in fast flowing liquid environment require surface topographies, which cause well-advanced cell attachment.

Therefore, it is of utmost importance to investigate not only the mechanical parameters of an a-SiC:H-MEMS-membrane but also the biocompatible characteristics of a-SiC:H with respect to cell attachment and proliferation. Furthermore, we will show that the switching behavior of a-SiC:H coated bistable membranes in liquids with viscosity values up to 286 mPa·s is possible, making buckled MEMS membranes applicable for experiments in medical liquids.

A. Membrane Technology

State of the art MEMS membranes exist in various geometries, offering a broad field of applications, ranging from porous separation membranes [28] over membranes as pressure-sensitive element [29]–[31] to buckled membranes. In the latter configuration they are the mechanically moving part within *e.g.* switches [32], valves [33] or ultrasonic transducers [14], [34]. To achieve a buckled state in a membrane requires a critical value of intrinsic compressive stress σ_c.

A detailed description of the term bistability as well as the corresponding potential energy split associated with the two resulting ground states is stated by Schomburg and Goll [35]. For a bistable switching procedure of buckled membranes, a mechanical stimulus is required. If an externally applied force exceeds a specific threshold [35], which is dependent of basic membrane properties, such as geometry and material composition, the membrane will switch from its current to its opposite ground state. Buckled membranes can be actuated via different mechanisms, such as hydraulically actuated hammer valves [36], pneumatically coupled membranes [33] or permanent magnets utilized in electromagnetic microrelays [37]. Dorfmeister *et al.* reported on micromachined membranes, which were excited by the piezoelectric effect [38]. The major advantage of this membrane actuation technique compared to those mentioned above is that the actuator is directly integrated on the membrane. Thus, an actuation cavity [33], [36] or external components such as magnets [37] are no longer needed. A precise description of a piezoelectrically initialized switching processes of bistable membranes in air is reported by Dorfmeister *et al.* [39]. Furthermore, piezoelectrically driven devices stand out with the striking advantage of comparatively low power consumption. Hence, this makes the piezoelectric technology very attractive for remote or mobile applications. To the best of our knowledge, so far only bistable MEMS membranes with integrated transducers, which are capable to switch in air have been reported in literature. Extending the application range of piezoelectrically actuated bistable membranes to liquid environments enables many exciting possibilities ranging from cycle controlled fluidic pumps over valve designs to microfluidic and biomedical applications.

To explore the potential of bistable membranes in the field of Bio-MEMS, the devices have to feature biocompatible properties required for intended application. Likewise, the implemented biocompatible properties must not interfere the mechanical bistable switching behavior.

B. Biocompatible Cell Environment

MEMS often consist of non-biocompatible materials inhibiting direct substrate to cell contact. In consequence an additional biocompatible layer must be applied on the substrate. A biocompatible possibility is crystalline silicon carbide, although it is difficult to integrate in the fabrication process. Therefore, we decided to investigate a-SiC:H as biocompatible material, because its thin film properties such as layer stress or hydrophilicity can be controlled (by deposition parameters) [25], [40]. The cell membrane has a surface charge, which results from the interplay of the membrane chemistry with its different types of charged amino acids and lipids with the resulting ion gradients generated by the cell's ion pumps between the intracellular and the extracellular space. Hence, it is reasonable, that the surface potential of a substrate plays a significant role for cellular attachment. Angelescu *et al.* [41] claim that the biocompatibility of a material is related to the materials electrochemical potential and that compared to pure silica surfaces a deposition of a thin carbon, or silicon carbide layer improves the biocompatibility for living cells. For this study we propose that compared to pure Si an increased carbon content is an advantage for the viability of human cells, so that a-SiC:H deposited with a higher carbon content is expected to display a higher biocompatibility compared to pure Si.

High requirements on the level of biocompatibility of a MEMS device emerge when the material is in direct contact with living tissue over an extended period of time. Hence,

to assess the biocompatibility, the evaluation of the proliferation, differentiation and adhesion of living human cells is a frequently used approach, that must be addressed to evaluate the safety as a pre-condition for progressive product development [42]–[44].

For assessing the biocompatibility of a-SiC:H, the adhesion and the proliferation of human Caco-2 cells on a-SiC:H layers was investigated. The Caco-2 cell line is an immortalized, adherent cell line derived from a human colon adenocarcinoma established in 1974 by J. Fogh [45]. Depending on the cell culture conditions, Caco-2 cells spontaneously differentiate and express several characteristics of the small intestine like tight junctions and apical microvilli [46], [47]. Therefore, the Caco-2 model is commonly used as an intestinal barrier model [46], [48]. Caco-2 cells are also frequently used in drug testing and toxicity studies [49], [50]. Furthermore, Caco-2 cells have already been used for biocompatibility and cytotoxicity assays [51], [52]. Attachment, growth and proliferation of Caco-2 cells are influenced by the material, structure and coating of the surface [53]–[55]. The attachment of Caco-2 cells can be supported by applying surface coatings containing fibrous proteins from the extra cellular matrix (ECM) or by changing the surface charge state by molecules. Wang *et al.* [55] has shown that Collagen type I, which is an ECM protein, and Poly-D-Lysine, which changes the surface charge condition, can significantly improve the attachment of Caco-2 cells on a polydimethylsiloxane (PDMS) surface compared to non-functionalized PDMS.

The typical growth process of Caco-2 cells shows a lag phase after seeding in which cell attachment to the surface takes place. This is followed by exponential cell proliferation towards an epithelial cell monolayer before a plateau is reached by confluency of the cell layer. The duration until a confluent cell layer is reached may vary in individual studies as it depends on multiple factors including the initial seeding density and the passage number of the used Caco-2 cell culture as reported by Briske-Anderson *et al.* [56].

In the present study the proliferation, viability and the adhesion of Caco-2 cells on a-SiC:H surfaces with different carbon concentrations were investigated. Additionally, the influence of Collagen and Poly-D-Lysine coatings was examined for different carbon concentrations of the silicon carbide layer. Targeting future biomedical applications this work addresses both the mechanical as well as the biological aspects of our a-SiC:H membranes. In this study we will describe the fabrication process of biocompatible bistable MEMS membranes, demonstrate successful bistable piezoelectric switching in liquid media and investigate the biocompatibility of a-SiC:H covered membranes. Such membranes provide surfaces with an environment for vital cell proliferation which can be mechanically excited, enabling aspired stimulated cell culture growth.

II. Experimental Details

A. Biocompatible a-SiC:H Layer Tuning

To gain knowledge of the degree of biocompatibility of the a-SiC:H coated membranes we performed cell culturing experiments on substrates with altered mechanical properties and biologically tuned a-SiC:H surfaces as described in the following section. For the plasma enhanced chemical vapor deposition (PEVCD) of the a-SiC:H thin films an Oxford Instrument PlasmalabSystem 100 with silane (SiH_4) and methane (CH_4) as precursor gases was used. The stress level of the thin films was controlled by the deposition parameters. As mentioned above, the stress window for buckled membranes has previously been carefully tailored: on the one hand the critical stress σ_c has to be exceeded, but on the other hand has to be close to σ_c, to keep the required force for switching low [22]. Thus, as compromise between these two requirements we targeted stress values of the a-SiC:H layer close to 0 MPa. According to [25] we set the closed-loop controlled substrate temperature at 25 °C, the RF plasma power to 800 W and the chamber back pressure at 30 mTorr. However, the film stress and the layer thickness were still influenced by the reactive gas flow ratio of the two precursor gases methane and silane

$$r_{CH4} = \frac{f_{CH4}}{f_{CH4} + f_{SiH4}} \tag{1}$$

whereby f_{CH4} and f_{SiH4} represent the gas flows of methane and silane, respectively.

As a first step and as part of the mechanical membrane characterization the residual stress of the different a-SiC:H layers was determined with the wafer bow method influenced by different deposition times ranging from 5 min to 10 min and gas flow ratios from 0.05 to 0.95 in varied in 13 steps, respectively. In a second step, the different surfaces were additionally treated with O_2-plasma for better hydrophilicity and hence, better cell adhesion [40], [57]. The samples were processed with a 150 W O_2-plasma at a substrate temperature of 25 °C and 150 mTorr for 5 min in an Oxford Instrument PlasmalabSystem 100 after a-SiC:H deposition. The altered hydrophilicity was measured by determining the contact angle with a Küsse DSA 30S setup.

Finally, the biological surface properties were modified using Collagen Type I (Sigma C7661-5MG) and Poly-D-Lysine (Sigma P7405) surface coatings. The surface coatings were deposited according to the recommendation of the manufacturer.

B. Cell Experimental Setup

A preliminary screening of the behavior of Caco-2 cells in terms of proliferation, adhesion and total cell count on different a-SiC:H thin films was performed, so that the results can indicate trends, but no statistically significant conclusion can be drawn from these results. Instead of investigating only few specific combinations in detail, we decided to design the experiment in a broader range to screen for the most influential parameters of a-SiC:H fabrication and post-treatment, in order to identify the most critical factor influencing the material's biocompatibility. The purpose was to reject or confirm several presumptions and to provide guidance for subsequent experimental planning.

For the characterization of the individual cell behavior the experiment was designed to be divided in three different parts,

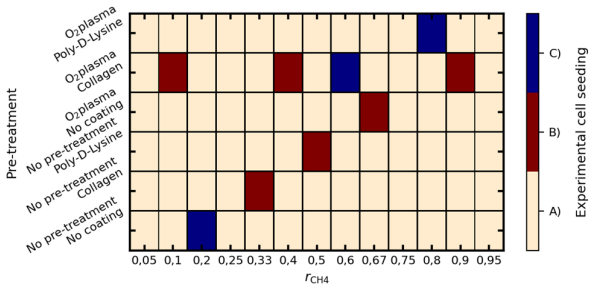

Fig. 1. Graphical representation of experimental design representing the different fabrication conditions of the a-SiC:H versus the applied pre-treatment procedure before cell seeding. A total of 78 individual surface modifications were cultivated for different types of investigations. All samples of A) were cultivated once for the total cell count after 120 hrs. Samples represented by B) were cultivated four times for the total cell count, proliferation and adhesion investigations. Samples marked with C) include all investigations of B) in addition of another cell culture for scanning electron microscopy (SEM) imaging. Figure 1 will further on act as a reference for a better overview in the details, as well as the experimental setup. Later, the experimental results (Figure 10) will be presented in the same graphical representation for better comparison.

consisting of (1) metabolic cell viability at 3 time points allowing to calculate the cell proliferation, and (2) the cell adhesion (Figure 1, red and blue samples) and finally (3) a total cell count after 120 hrs (Figure 1, all samples). The metabolic viability measurements (1) took place 72, 96 and 120 hrs post seeding of Caco-2 cells on to the a-SiC:H surfaces, while the adhesion investigation (2) and counting of the total cell number (3) were conducted at day 5 (in vitro) post seeding, where typically already a dense cell layer can be reached. A schematic overview of the experimental design and of the cell culturing scheme is displayed in Figure 1.

For cell culture preparations all samples were sterilized with 70 % ethanol and placed inside 24-wellplates prior cell seeding. The growth medium consists of Minimum essential medium (MEM) (Sigma) supplemented with 20 % Fetal Bovine Serum (FBS) (Sigma), 1 % Penicillin and Streptomycin (Sigma), 1 % Sodium Pyruvate (Sigma) and 1 % L-Glutamine (Sigma). The cells are seeded at a density of 50.000 cells per well and the total amount of growth medium was 1 ml per well. Incubation took place at 37 °C and 5 % CO_2.

The viability of the cells was examined using a PrestoBlue© assay after 72, 96 and 120 hrs (first (1) and third (3) part of the cell experiment). PrestoBlue is a cell viability reagent based on resazurin, which is cell permeable and reduced to resorufin by metabolic active cells. When PrestoBlue is added to the media the reduction inside the cells leads to a change of the mediums absorbance and fluorescence, which is proportional to the number of active metabolic cells [58]. After addition of PrestoBlue, the cells are incubated for 30 min, before 100 μl of the supernatant is pipetted to a fresh well plate. A PerkinElmer© EnSpire 2300 plate reader was used to measure the reduction of the PrestoBlue giving a proportional number to absolute cell count. A normalization with the cell count of a silicon reference sample allows to provide a relative cell count from 0 (no viable cells) to 1 (as much metabolism as on the reference sample) as silicon is considered to be a biocompatible material [59]. Subsequent to the proliferation test, optical adhesion inspection was performed with the same batch of cells.

In the second part of the experiment the adherent cells were detached from their substrate by adding 500 μl trypsin to each well. After 5 min $\pm$0.5 min the trypsin was inactivated by adding 500 μl of fully supplemented growth medium. The trypsin-media-mix was carefully removed and subsequently the substrate was rinsed carefully by slowly adding phosphate buffered saline (PBS) to the rim of the well plate avoiding shear stress to the still attached cells. The PBS rinsing step is carried out two more times, rechanging the PBS prior to each step. We propose that with confluent cell layers and strongly attached cells this enzymatic dissociation is slower than with patched cell layers of weakly attached cells. Hence, we suggest that the amount of cells still attached to the surface after a precisely defined trypsinization duration can also be interpreted as qualitative cue for the relative biocompatibility of the corresponding surfaces.

The cells, which are remaining on the substrate were stained with Fluorescein Diacetate (FDA). FDA is a cell permeable stain and hydrolyzed to fluorescein, which is fluorescent, in cells with an active metabolism. In consequence, only living cells get excited in the fluorescence microscope [60]. The pictures of FDA-stained cells were taken with a fluorescence reflected light microscope (LEICA DM6000) and a LEICA DFC 420c camera system. To confirm the obtained adhesion results a second batch of cell cultures (Figure 1, red and blue samples) underwent the process of a wash assay [61] after 120 hrs. Hereby, the cells were carefully flushed off manually with 100 μl of MEM using a 1 ml pipette. Cells, which were remaining on the surface after the washing step were also stained with FDA and pictured as described above.

Finally, for a detailed microscopic investigation by electron microscopy the Caco-2 cells were grown on a specific selection of three different surfaces (Figure 1, blue samples) for five days. The attached cells were primary fixed using a mix of 2 % Paraformaldehyde (PFA) and 2.5 % Glutaraldehyde (GA) in 500 μl of PBS. For dehydration of the fixed sample an Ethanol (EtOH) grade series with 35 %, 50 %, 70 %, 95 % and three times 100 % is used for 10 min each. Chemical drying is performed by adding a 1:1 mix of EtOH and Hexamethyldisilazane (HMDS) followed by two times 100 % HMDS with an incubation time of 5 min each. After incubation the HMDS is discarded and the cells were dried at room temperature. The dried samples were examined by scanning electron microscopy (SEM) using a 5 kV electron beam of a Zeiss Neon Crossbeam system.

C. Biocompatible Membrane Switching Setup

An important part of this work was to sustain a sufficient biocompatibility of such a-SiC:H layers, while maintaining the initial functionality of the MEMS device for bistable switching operation. For this purpose, we utilized buckled MEMS membranes with integrated piezoelectric transducers. These membranes were fabricated with diameters ranging from 600 μm to 800 μm and a thickness of 3.3 μm$\pm$0.1 μm. These

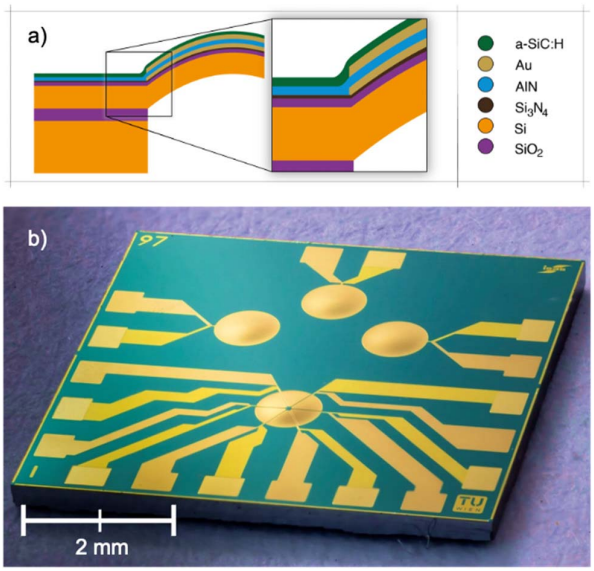

Fig. 2. a) Schematic cross-sectional view of a biocompatible piezoelectric bistable membrane with a thin layer structure of 1.3 μm on top of a 2 μm thin silicon membrane. In b) an optical micrograph shows four membranes each with 700 μm diameter on a 6 $\times$ 6 mm^2 chip. It can be seen that the electrodes to excite the membrane can be fabricated in different designs enabling a tailored electrical excitation pattern. Within the scope of this work, we investigated only the full covering electrode design as represented by the upper three membranes.

dimensions were previously investigated as the sweet spot to show buckling behavior and to enable bistable switching [22]. The gold electrodes to excite the piezoelectric transducers were deposited by thermal evaporation, while the piezoelectric aluminum nitride (AlN) layer was synthesized by reactive DC magnetron sputtering. A detailed description of the fabrication process is given in [38].

As already mentioned, the required effective stress to buckle the membranes in order to achieve bistable switching behavior had to be set precisely within a certain range. That range was determined by the membrane dimensions and was reached with the AlN layer at $\sigma_{\mathrm{AlN}} = -600$ MPa ± 60 MPa. After the evaluation of all three parts of the cell experiment we covered our bistable membranes with an a-SiC:H layer specifically chosen as described below. The results obtained from both, the cell experiment and the mechanical stress analysis were considered to select an a-SiC:H layer with intended biocompatible properties such as low adhesiveness and high cell proliferation for cell experiments with mechanically oscillating surfaces while simultaneously maintaining bistable switching of the MEMS membranes. The desired a-SiC:H layer was deposited on top of the existing layer stacking with a residual stress of $\sigma_{\mathrm{SiC}} = -170$ MPa ± 25 MPa and a layer thickness of 70 nm ± 3 nm. The thickness was chosen as a good agreement of closed layers, which were also as thin as fabricable and measured optically by a Filmetrics© F20-UVX thin film analyzer. A schematic cross-sectional view as well as four representative membrane devices are illustrated in Figure 2.

In order to switch the biocompatible and bistable membranes, an electronic setup scheme was installed as shown in Figure 3.

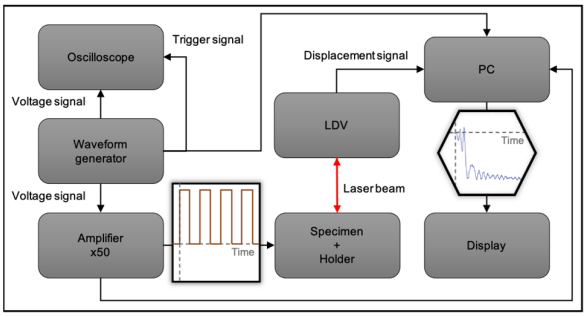

Fig. 3. Excitation scheme to initiate a switching procedure. The membranes were optically monitored with a laser Doppler vibrometer (LDV), while excited electrically with a tailored voltage stimulus. Due to the individual response of the membranes, the amplitude and duration of the rectangular signal was customized until a switching operation was achieved. Specific displacement pattern gave tendencies to alter the excitement parameters in order to maximize the dynamic membrane amplitude and ultimately initiate a bistable switching procedure.

TABLE I
FLUID PROPERTIES OF THE USED TEST LIQUIDS

Fluid	Dynamic viscosity [mPa·s]	Density [g/mL]	Temperature [K]
ISO	2.19	0.785	293
D5	5.51	0.840	293
N10	17.53	0.846	293
N35	71.96	0.855	293
N100	286.10	0.866	293
D500	713.40	0.872	293

As a first step the membranes were stimulated with a 0.3 V 0 – 350 kHz periodic chirp signal to measure the resonance frequency of the fundamental vibration mode f_{res1} in air in order to determine switchable membranes. The second step was to induce switching of the membranes in fluids. To excite our membranes we used pulsed DC rectangular signals with individual switching frequencies f_{switch} of $\sim$8 kHz below f_{res1} pictured in Figure 3 and discussed in more detail in [24]. For clarification it should be noted that f_{switch} is the frequency at which a membrane switches from one ground state to its opposite state. To cover a broad range of possible fluidic applications we used liquids from Paragon-Scientific with dynamic viscosities ranging from 2.2 mPa·s up to 713.4 mPa·s. A list of the corresponding liquids is given in Table I. To initialize a switching of a membrane immersed in a liquid the interaction of excitation voltage, burst count and frequency must be carefully selected. Each membrane was characterized with respect to its individual switching behavior, resonance frequencies f_{res1}, maximum membrane center velocity v_{res1} at f_{res1} and switching frequencies, respectively.

III. RESULTS

A. Cell Observation Results

As a part of the a-SiC:H thin film characterization the wettability was first investigated. The contact angle θ was influenced by the corresponding carbon content, which is directly correlated to r_{CH4}, of each sample and whether the

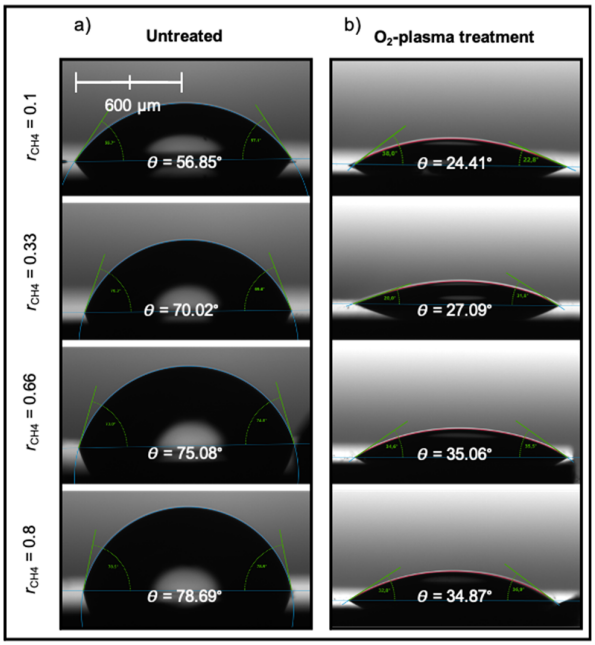

Fig. 4. Four representing a-SiC:H surfaces with increasing carbon content were investigated in terms of wettability. Increasing carbon content of the layer results in a more hydrophobic surface, which can be seen in a). In b) the additional O_2-plasma treatment leads to an oxygen terminated surface, which increases the hydrophilicity of the a-SiC:H surface.

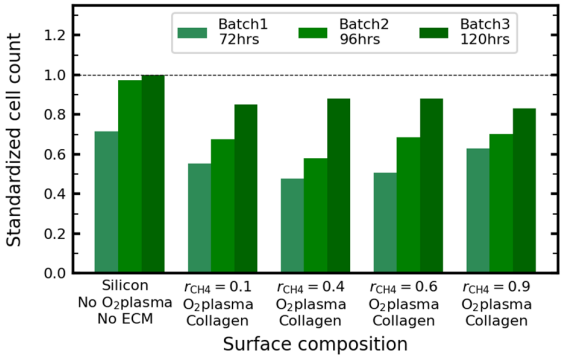

Fig. 5. Comparison of cells grown on different a-SiC:H thin films with O_2-plasma pre-treatment *and* Collagen coating and silicon as a reference. The viability of cells was determined by PrestoBlue assay at 72, 96 and 120 hrs after seeding. A high viability correlates to a high cell count. A-SiC:H-values were normalized to the cell count on Si reference samples.

surface was O_2-plasma treated or not. Figure 4 a) gives an impression of the increasing θ of a 2 ml water droplet on a-SiC:H surfaces with increasing r_{CH4}. Figure 4 b) reveals an average decrease of the contact angle of $\Delta\theta = 39.8°$ after an O_2-plasma treatment for 5 min duration, which led to oxygen terminated surfaces.

The significant decrease of the contact angle with r_{CH4} indicates an increasing hydrophilicity due to the O_2 plasma treatment, overcompensating the intrinsic hydrophobicity of the a-SiC:H layer. We assume, that the O_2-plasma oxidized the surface of the a-SiC:H and reduced the carbon-level at the very surface while leaving the Si in an oxidized state, thus resembling a SiO_2-like surface, thus, enhances cell adhesion and growth [57].

Next, we investigated the proliferation rate on different a-SiC:H surfaces as the first (1) part of the cell experiment. Human Caco-2 cells were seeded on untreated (as-is) surfaces as well as on pre-treated surfaces. The cell proliferation and their adhesion to the surface were investigated as previously described in II. B. A cell viability test performed with an optical plate reader was used to interpret the cell number: A high signal intensity correlates with a high cell number of viable Caco-2 cells. An increase of the viability value with progressing culturing time (from 72 hrs to 120 hrs in vitro) can be interpreted as an increase in cell number (*i.e.* cell count) and indicates a good cell proliferation on this surface. This interpretation concerning the cell number is also supported by optical microscopy results of the Caco-2 coated surfaces. The viability values were normalized versus the values obtained on pristine ("no O_2-plasma – no ECM coating") Si-wafers with an intrinsic SiO_2 surface, which is known to be a biocompatible material [44].

Results for (i) pristine a-SiC:H surfaces, (ii) only O_2-plasma treated surfaces and (iii) only ECM coated surfaces without plasma treatment showed low and inconsistent viability values (not shown), indicating an unreliable proliferation of these surfaces. Only for a-SiC:H surfaces, that were dually pre-treated with both, an O_2-plasma and a Collagen Type I coating resulted in an monotonously cell grow over time and a cell viability that was almost as high as that of pure Si surfaces with the biocompatible SiO_2 surface [44]. The relative cell count on four a-SiC:H samples fabricated with a different r_{CH4} ranging from 0.1 to 0.9 and on silicon is illustrated in Figure 5.

All a-SiC:H surfaces portrayed in Figure 5 were dually pretreated with O_2 plasma and Collagen Type I coating. Despite the different carbon contents of these dually pretreated surfaces displayed no significant difference for the biocompatibility with different r_{CH4}-ratios. Optical microscopy of these samples confirms, that after 120 hrs in vitro the cell layer was already close to or approaching confluency, *i.e.* a 100 % surface coverage with living Caco-2 cells. This permanent increase of the cell number on the surface between 72 hrs and 120 hrs is an indicator of a sufficient biocompatibility, that is well comparable to the biocompatibility of SiO_2 [44]. We propose that due to the dual pre-treatment all surfaces regardless of their Si to C-ratio could be made biocompatible. The operation of MEMS devices pre-treated with this process is fully maintained.

Figure 6 visualizes the same four samples used to generate the data for Figure 5. The surfaces with the fluorescent stained cells were image after 72, 96 and 120 hrs of growth, giving a qualitative optical confirmation of the conducted cell growth over time. Optical inspection revealed that the proliferation rate of the cell cultures was different within the first days, and some cell cultures were proliferating faster than others. The images in the right column (120 hrs) of Figure 6, however, indicate, that despite the different r_{CH4}-values of the a-SiC:H surfaces after 120 hrs all cell layers on dually pre-treated surfaces were already close to 100 % confluence. Differences in the initial growth rates disappeared with longer culturing

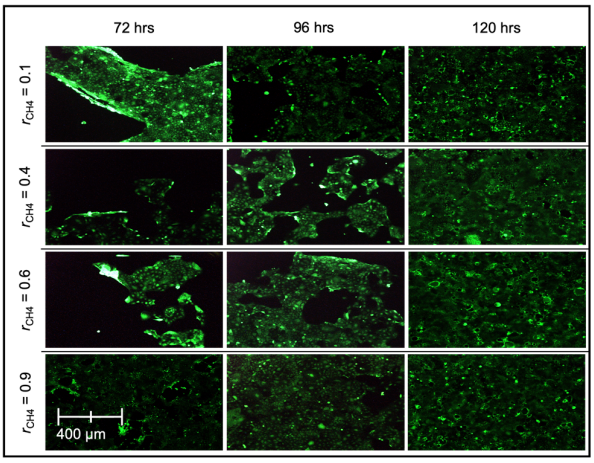

Fig. 6. Optical representation of the cell proliferation of the same four a-SiC:H surfaces of Figure 5 treated with O_2-plasma *and* Collagen coating photographed with a fluorescent microscope and a LEICA camera system under 200 times magnification. FDA-stained cells were imaged after 72, 96 and 120 hrs in vitro. The observed differences in cell proliferation confirmed the cell count of Figure 5. (Note: The images show the least cultured part of each sample).

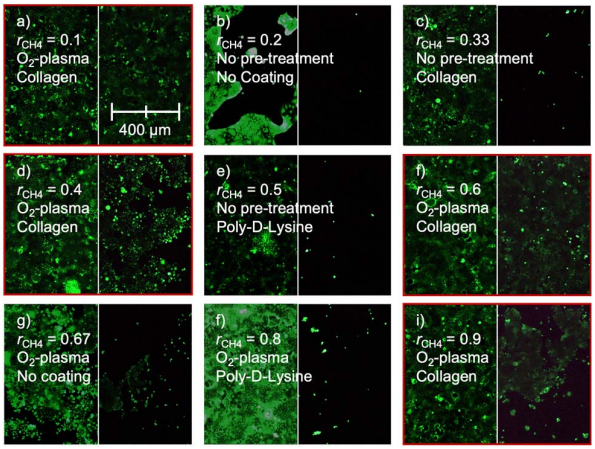

Fig. 7. Optical images of nine a-SiC:H surfaces (a–i) with FDA stained Caco-2 cells after 120 hrs of growth time. Each image shows a comparison of cells on the sample before (left side) and after (right side) five minutes of trypsinization. Again, only the dually pre-treated a-SiC:H surfaces (a, d, f, i) showed a significantly better attachment of the cells on the substrates. No correlation with the stepwise increased gas flow ratio from $r_{CH4} = 0.1$ to 0.9 was observed. (Note: The taken images show the most populated areas on the sample and are only indicative results).

time. These observations agree with the Presto Blue viability assay displayed in Figure 5.

As the second (2) part of the cell experiment the adhesion on different a-SiC:H surfaces (Figure 1, red and blue samples) was qualitatively characterized with previous described assays. Therefore, the ratio of detached and remaining cells was determined as a qualitative indicator for the adhesiveness of Caco-2 cells on their individual surface. The first assay was to loosen the cells from the substrate by trypsinization. The impact of different surface properties and pre-treatment procedures is shown in Figure 7. Only cells grown on O_2-plasma pre-treated *and* Collagen coated a-SiC:H surfaces showed a comparatively high Trypsin resistant behavior, compared to other surfaces

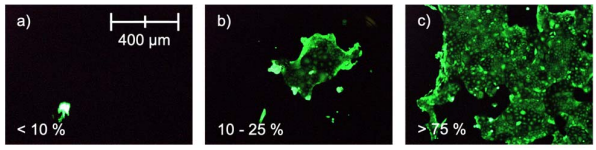

Fig. 8. Representatively selected images of remaining cells on the sample after a wash assay. The number of FDA stained Caco-2 cells were determined optically and classified in a) "low", b) "medium" and c) "high" numbers of residual cells. An improvement in cell attachment was only observed on O_2-plasma pre-treated *and* Collagen coated a-SiC:H surfaces. Only those samples could be classified as "high". Different gas flow ratios from $r_{CH4} = 0.1$ to 0.9 of the a-SiC:H layer were also taken into account but did not affect the adhesiveness.

that had either not undergone O_2-plasma pre-treatment, or no collagen coating (Figure 7 b, c, e, g, f).

This preliminary result indicates that – irrespective of the a-SiC:H fabrication – the surface treatment with O_2-plasma *and* Collagen coating elevates the adhesion properties of the surfaces to the cells. Only this specifically treated surface provided the necessary environment, so that even the enzymatic procedure of trypsinization left the cells to some extent unaffected for the limited period of 5 min. This finding can also be interpreted as an increased stability against trypsin provided by the enhanced surface properties for cell adhesion.

To reinforce these results, a wash assay was performed. Doing so, the cells were carefully rinsed off the surface, so that shear stress created by the flow working on the adherent cells was kept at a minimum. The remaining cells, which were still attached to their surfaces after the wash assay were imaged and categorized as illustrated in Figure 8. The number of cells still attached after a consistently conducted washing procedure was interpreted as an indicator for the adhesiveness of the surface for epithelial cells and stand in good agreement with the results of the cell loosening assay with trypsin. In both experiments the r_{CH4} of the a-SiC:H layer did not influence the adhesiveness. Similar to Figure 7 b) surfaces with no O_2-plasma treatment and no ECM showed the weakest adhesiveness and were categorized with "low" ($<$10 % remaining cells), as displayed in Figure 8. The highest adhesiveness with a remaining confluence in the range of 75 % and above was observed for O_2-plasma pre-treated *and* Collagen coated a-SiC:H surfaces. Only these samples were categorized as "high", indicating their improved adhesion properties. Every other combination of various surface modifications was classified as "low" or "medium" with maximum 25 % remaining cells on the substrate. (No surface was investigated with remaining cells between 25 % and 75 %.)

To investigate the increased adhesiveness of Caco-2 cells on O_2-plasma pre-treated *and* Collagen coated a-SiC:H surfaces, a SEM analyses was performed. In Figure 9 a) a prominent cell on an O_2-plasma pre-treated *and* Collagen coated a-SiC:H surface with $r_{CH4} = 0.6$ can be seen (see also Figure 1, blue samples). The cells have been fixed to maintain their original morphology throughout the subsequent drying caused by the SEM vacuum chamber. The SEM image illustrates a flattened and spread out cell, which indicates an adhesive binding to the surface. In Figure 9 b) a higher magnification reveals an

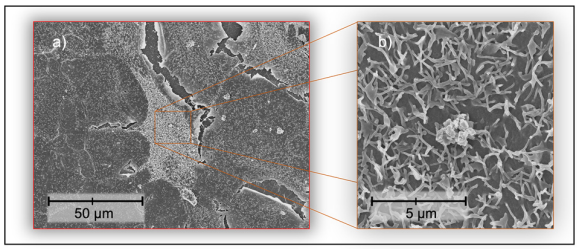

Fig. 9. SEM images of a prominent cell under a) 2000 and b) 20000 times magnification after 120 hrs. The surface was pre-treated with O_2-plasma *and* coated with Collagen and the a-SiC:H thin film was deposited with a gas flow ratio of $r_{CH4} = 0.8$. The cell appears spread-out and flattened. At higher magnification (b) also the microvilli become visible. Microvilli are a specific feature of Caco-2 cells and indicate good differentiation and good adhesion between cell and substrate surface.

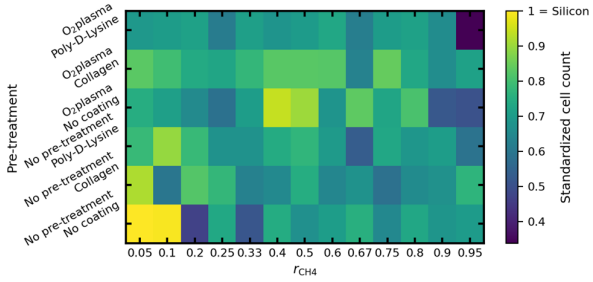

Fig. 10. Final cell count after 120 hrs via PrestoBlue assay, carried out with a PerkinElmer EnSpire 2300 plate reader. This method provides as a result an equivalent and linear proportional number, representing the absolute cell count. For better presentation, the numbers were set in relation to the count on silicon. The graphic illustrates, how the mechanical and biological properties of the modified a-SiC:H thin layers influenced the cell proliferation on such different surfaces independently of one another. This plot represents the actual results of the experimental approach presented in Figure 1.

increased number of microvilli, which is indicative for good differentiation of the cell on the surface, explaining the wide spread of the cell. Surfaces which force such an interaction of cells with their environment are considered as most viable surroundings for cells [62].

The following section contains the results of the final cell count as the third (3) part of the cell experiment. After a total growth period of 120 hrs on the a-SiC:H surfaces a final PrestoBlue viability assay was performed. The increase of the viability readout to previous measurements allows to assess the proliferation of cells and correlates with the total cell count on the surface. The optical readout of the fluorescents emissions of all samples was normalized to a pristine silicon sample acting as reference sample. The normalized adsorption of PrestoBlue in all 78 samples (see Figure 1) is proportional to the number of living cells and illustrated in Figure 10. The x-axis pictures the variation of the carbon content of the a-SiC:H thin films represented by an increasing r_{CH4}, assumingly influencing the cell count with altered hydrophilicity [40], [57] as well as electrochemical surface potential [41]. As shown in Figure 4, the hydrophobicity increases due to an increased carbon content controlled by r_{CH4}. On the y-axis the impact on the biological properties of the surfaces, caused by treatments such as O_2-plasma and different ECMs, is given. Two local maxima can be spotted at $r_{CH4} = 0.05$ and $r_{CH4} = 0.4$. The first maximum is the sample with no surface modification, an assumably very low carbon content, close to pure silicon and therefore an almost unchanged surface wettability. The numbers of the untreated a-SiC:H samples with low carbon content matched well with the cell counts on pure silicon with a normalized cell count of 0.995 for a-SiC:H. The second maximum was triggered by surfaces only treated with O_2-plasma and without any ECM. Giving these conditions, the nominally increased carbon content [25] leads to a more hydrophobic surface (Figure 4). This second maxima stands in good agreement with literature [41], that cells tend to favor surface materials such as carbon with +0.33 mV, which are close to their electrochemical potential. Above a gas flow ratio of $r_{CH4} = 0.6$ Figure 10 shows a decline in cell population due to the high hydrophobic characteristic of the surfaces. Surfaces, which were pre-treated with the O_2-plasma indicated a higher tendency for an increased cell proliferation. It should be mentioned, that a three times lower contact angle does not mean three times higher cell proliferation, however an increase in cell numbers was detectable. The increased hydrophilicity and enhanced carbon content led to a local maximum at $r_{CH4} = 0.5$.

B. a-SiC:H MEMS Application

The biological pre-investigation about the a-SiC:H layers was necessary to ensure biocompatibility. For fluidic valve applications, this requests easily detachable cells and high proliferation. According to the cell adhesion investigations, the lowest cell attachment appeared on untreated a-SiC:H thin films without ECM coating. Furthermore, the highest cell proliferation was found at $r_{CH4} < 0.3$. In addition to the biological properties it was of major interest to minimize the impact of this layer on the bistable characteristics of the membrane. Therefore, the layer thickness was kept as thin as possible.

The following measurements were conducted to evaluate, which had the lowest mechanical impact on our buckled membranes. Figure 11 a) displays the thickness of the thin films as a function of deposition time and gas flow ratio r_{CH4}. It is also shown in Figure 11 b) that the increasing compressive stress with increasing carbon content is almost independent from layer thickness up to a gas flow ratio of $r_{CH4} = 0.67$. To select a thin film transferring minimal mechanical stress to the membrane at low layer thicknesses, but guaranteeing a complete coverage of the surface topography, the four most promising layer compositions were selected. These thin films A – D were deposited on five membranes each and are given in Figure 12. The membrane deflection under a sinusoidal stimulus of 5 V at 2 kHz was measured in air both, before and after thin film deposition. The resulting amplitudes were normalized in relation to the initial amplitude without an a-SiC:H layer. The resulting deviation is a direct measure of the influence of the altered layer stacking. From that point on membranes were for further characterization only coated with thin film "C", a 70 nm ±3 nm thick a-SiC:H layer with a residual stress of $\sigma_{SiC} = -170$ MPa ±25 MPa. This

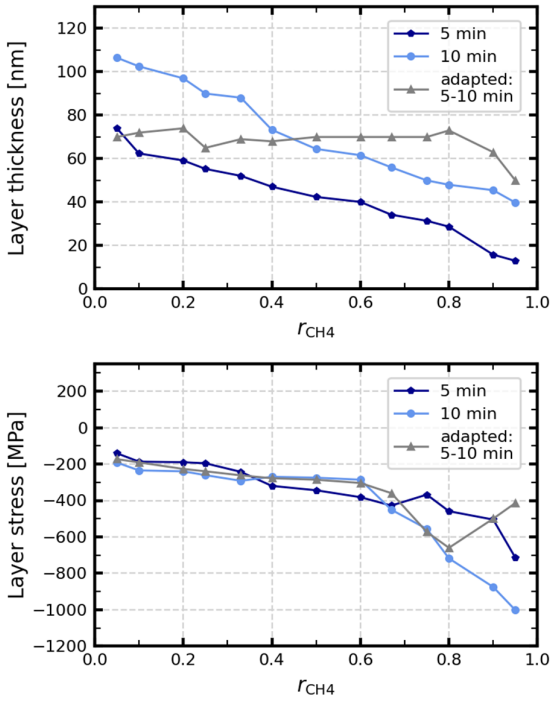

Fig. 11. A biocompatible a-SiC:H layer was investigated in terms of layer thickness and residual stress, depending on the deposition time and different silane to methane gas flow ratios r_{CH4} (T = 25 °C, P_{plasma} = 800 W, p = 30 mTorr). Because of the stress dependency from the layer thickness, it was the goal to achieve constant layer thicknesses of 70 nm ±3 nm. Therefore, the deposition time was adapted from 5 to 10 min starting at r_{CH4} = 0.05 with 5 min and was stepwise increased until r_{CH4} = 0.95 and 10 min (grey line). The inserted lines only serve as guide to eye.

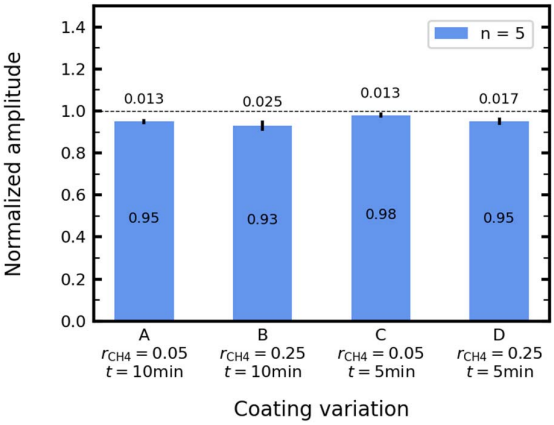

Fig. 12. Five membranes were coated with four different a-SiC:H layers, respectively. The initial vibration amplitude of the membrane in air is marked in the chart at 1.0. A decrease of the amplitude after thin film deposition was observed compared to the initial membrane amplitude under a 5 V sinusoidal stimulus. The error value for each coating is printed above its corresponding bar. Coating C influenced the vibrational behavior the least and was also the most consistence in terms of repeatability.

additional deposition led to an increase of the first resonance frequency f_{res1} by 2 kHz, which is important, when it comes to membrane switching.

C. Liquid Switching Measurements

In total 30 MEMS membranes were subsequently covered with an a-SiC:H layer to guarantee biocompatibility.

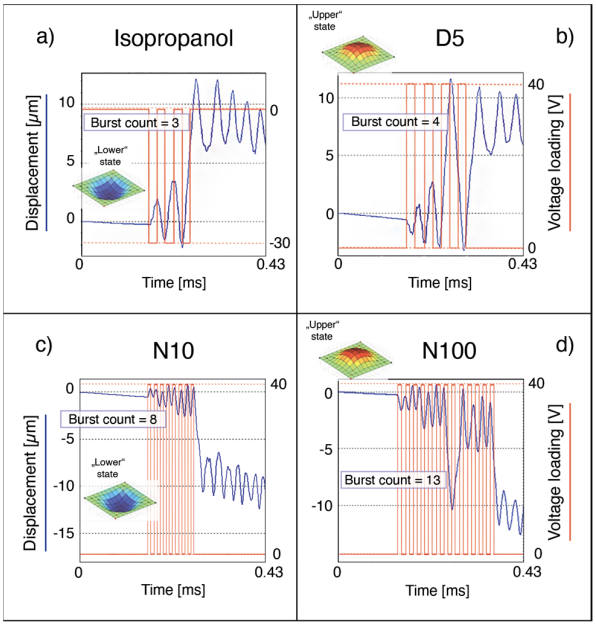

Fig. 13. LDV recording of bistable switching procedures from the "lower" to the "upper" ground state (a, b) or *vice versa* (c, d). Each figure represents an increasing viscosity and illustrates its direct effect on the switching behavior of the membrane. In a) 3 bursts and 30 V were necessary to initiate a bistable switching procedure, while in b) the burst count was 4 and the voltage level increased to 40 V. A further increase of required pulses can be seen in c) and d). Exceeding a viscosity level of N100 no further switching was detected. (Note: A linear drift of the displacement measurements occurred, because of the quantification and integration of the measured velocity.)

The membranes were introduced in the measurement setup as shown in Figure 3. As reported in [24] it is important to cover not just the top surface of the membranes with the test liquids, but the whole device. Otherwise, surface tensions of the liquid led to a drift of f_{res1} towards f_{res1} in air and made a precise determination of the resonance frequency impossible. The membranes were stimulated with individually tailored rectangular pulses and their switching behavior was characterized. Initially, 60 % of the tested membranes showed bistable switching in air. The percentage decreased to about 33 % after immersion in isopropanol, which was the testing liquid with the lowest viscosity. The percentage decreased further until only a single membrane was capable of bistable switching at a high viscosity of 286 mPa·s. When increasing the viscosity of liquids, initially bistable switchable membranes started to exhibit monostable behavior until no switching could be achieved. A monostable membrane is able to switch into its second ground state, but does not remain in the latter state, but switches back instantaneously. The change from bistable to monostable to no switching occurred monotonically with increasing viscosity for all membranes. [24]

To determine if a membrane has the intrinsic ability for bistable switching and how to predict this feature, optical measurements of a membrane movement during a switching procedure in four different viscous liquids were performed as illustrated in Figure 13. With increasing viscosity, it becomes more difficult to initiate membrane switching. This was reflected in the corresponding electrical parameters

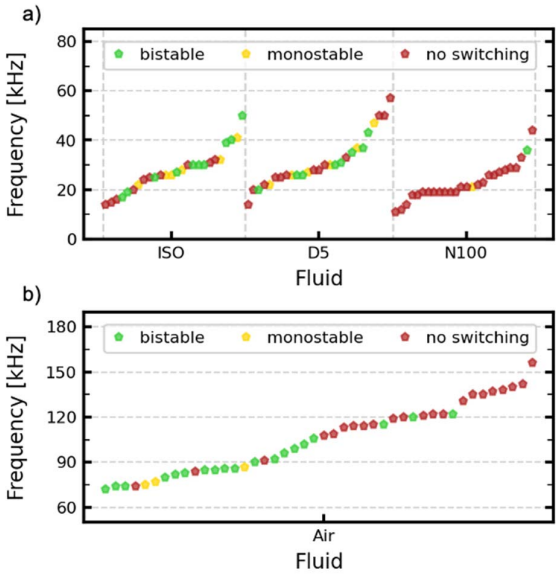

Fig. 14. Graphic representation of the resonance frequency f_{res1} in each selected fluid and the related type of switching of the tested membranes. The frequencies are displayed in ascending order, whereby in a) no pattern in terms of switchability could be observed. b) compares the same measurement of membranes in air, revealing a higher chance to show bistable switching behavior the lower f_{res1} was.

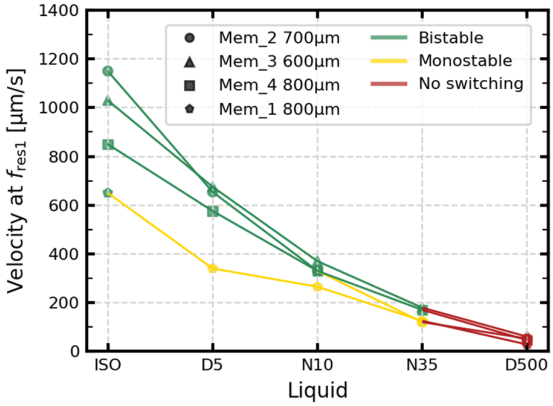

Fig. 15. Four representative membranes showing a decrease of the membrane center velocity v_{res1} under a 0.3 V periodic chirp signal at f_{res1}. This occurred as expected due to an increase of the viscosity. Falling below of a specific threshold in each fluid indicated an increased probability not to achieve bistable switching anymore.

such as burst counts and voltage level, but not in frequency. In Figure 13 a) an almost ideal switching procedure is shown. Hereby 3 pulses with an amplitude of 30 V initiated switching. Membranes that could be switched with similar parameters were likely to be also capable of bistable switching in higher viscous testing liquids. Due to the higher viscosity the fluidic resistance increased and more energy was required to initiate a switching process (see Figure 13 b) – d)). This resulted in higher voltage levels up to 45 V as well as up to 13 pulses. A further increase of the viscosity resulted in the membranes either showing monostable or no switching behavior at all. Increasing the voltage extended the viscosity range, in which bistable switching could be triggered. Exceeding the voltage level of 45 V caused damage to the piezoelectric transducer elements and thus sets an upper limit on the viscosity, in which switching is possible.

The observation of the switching capability with an LDV was a qualitative approach to estimate the basic behavior. The obvious disadvantage of this method is that the changing switching behavior does not lead to a quantitative prediction. To provide a small signal analysis method, we investigated correlations between other characteristic membrane properties and its switching ability. In [24] we showed that the deflection height was independent from the switching parameters due to given static potential energy well of the two ground states. Also, the resonance frequency f_{res1} in each testing liquid gave no indication, if a membrane is able to switch.

Figure 14 illustrates f_{res1} of the membranes in three representative liquids covering a large viscosity range and in air, respectively. The switching behaviors in liquids point out an independency of the switching capability and f_{res1}. Compared to that, in Figure 14 b) can be seen that f_{res1} in air provided information with 90 % accuracy [24], if a membrane achieves bistable switching or not. Nevertheless, the frequency f_{res1} depends on the density of the liquid. This was shown by a linear regression of f_{res1} of all measured membranes in each testing liquid shown in [24].

As a final characteristic measurement, we determined the membrane center velocity v_{res1} at its resonance frequency f_{res1}. Figure 15 provides information of the membranes' v_{res1} in each liquid, correlated with the information of switching capability, respectively. The increasing viscosity suppressed the movement of the membrane, resulting in decreasing v_{res1}.

Figure 15 gives a tendency for a threshold for a required v_{res1} to achieve mono- or even bistable switching. To the best of our knowledge this parameter was the only one, which concludes to a predictive behavior of a membrane's switching capability in liquids. The deviations between individual membranes originated from local inhomogeneities, such as film stress and membrane thickness.

IV. Conclusions

In previous works purely electrical low-power switching of bistable membranes was demonstrated in air [14], [38], [39] and in different fluids with viscosities up to 286 mPa·s [24]. To expand the field of applications of such membranes to biomedical applications a cell experiment was conducted using Caco-2 cells. Several different a-SiC:H thin layers with different carbon contents were chemically (O_2-plasma) and/or biologically (protein coating/surface charge) modified and investigated in terms of changes of their biocompatibility and cell adhesion. Hydrogenated amorphous silicon carbide surfaces of any carbon content pre-treated with a 5 min O_2-plasma *and* coated with Collagen Type I representing the ECM component featured a substantially enhanced adhesiveness compared to any other surface modification given in Figure 1. This is considered a notable improvement of the surface properties. In addition, the cell growth over time was the more stable and more homogeneous on these surfaces compared to other modifications. Based on our preliminary findings we propose that the contact angle as measure of the

hydrophobicity of a surface is also associated with the cell adhesion and cell proliferation on such surfaces. To screen basic properties, 78 mechanically varying a-SiC:H thin films were biologically modified and cultured with Caco-2 cells for 120 hrs. The motivation for this series of experiments was to identify a potential influence of the carbon content and of the impact of different surface pre-treatments on the cell proliferation and adhesiveness. The results of preliminary experiments revealed that existing devices can be additionally covered with an a-SiC:H layer with carefully selected parameters, depending on specific application requirements. Most important we showed that the a-SiC:H layer can be individually designed in terms of stress level, cell proliferation and cell attachment independently of each other, giving access to a broad field of application.

We proved this by covering bistable piezoelectric membranes with an unmodified a-SiC:H layer with low carbon content. We choose this specific layer composition for good cell proliferation, but low cell adhesiveness and a low stress level. This was to minimize any mechanical impact due to the additional coating on the final device's performance. To give another bistable membrane application, the impact of high acceleration on cells could be a potential field of investigation [63]. In this case, the a-SiC:H coating would be designed for best cell attachment as well as proliferation.

A qualitative estimation for the switching behavior of the membranes was presented, depending on the changing switching parameters and the related viscous fluid. Furthermore, a direct connection of the membrane center velocity v_{res1} and the corresponding switching ability was pointed out. This approach enables a small signal analysis method to assess bistable switching in liquids for MEMS membranes.

The biocompatible membranes showed bistable switching behavior up to a dynamic viscosity of 286 mPa·s. This value exceeds the viscosity of *e.g.* blood with 4.2 mPa·s [64] or the viscosity of typical MEM solutions with 1.050 mPa·s $\pm$0.027 mPa·s [65] by far. As a result, such membranes are now available for cell experiments in fluidic environments with controllable mechanical excitation of highly biocompatible surfaces.

ACKNOWLEDGMENT

The authors would like to thank DI Markus Pribyl (TU Wien) for taking and providing SEM pictures of preserved Caco-2 cells on different substrates.

REFERENCES

[1] D. L. Polla *et al.*, "Microdevices in medicine," *Ann. Rev. Biomed. Eng.*, vol. 2, no. 1, pp. 551–576, 2000.

[2] D. L. Polla, "BioMEMS applications in medicine," in *Proc. Int. Symp. Micromechatronics Hum. Sci.*, Sep. 2001, pp. 13–15.

[3] A. D. DeHennis and K. D. Wise, "A fully integrated multisite pressure sensor for wireless arterial flow characterization," *J. Microelectromech. Syst.*, vol. 15, no. 3, pp. 678–685, Jun. 2006.

[4] R. A. Scheidt *et al.*, "Microchips as implantable drug delivery devices," in *Proc. 1st Annu. Int. IEEE-EMBS Special Topic Conf. Microtechnol. Med. Biol.*, Oct. 2000, pp. 483–486.

[5] J. T. Santini, Jr., A. C. Richards, R. Scheidt, M. J. Cima, and R. Langer, "Microchips as controlled drug-delivery devices," *Angew. Chem. Int. Ed.*, vol. 39, no. 14, pp. 2396–2407, Jul. 2000.

[6] B. Ma, Z. Gan, and S. Liu, "Flexible silicon microneedles array for micro fluid transfer," in *Proc. 6th Int. Conf. Electron. Packag. Technol.*, Aug./Sep. 2005, pp. 1–5.

[7] Z. Xu *et al.*, "An integrated intelligent insulin pump," in *Proc. 7th Int. Conf. Electron. Packag. Technol.*, Aug. 2006, pp. 1–5.

[8] K.-S. Teh, Y.-T. Cheng, and L. Lin, "Nickel nano-composite film for MEMS applications," in *12th Int. Conf. Solid-State Sens., Actuators Microsyst. Dig. Tech. Papers*, vol. 2, Jun. 2003, pp. 1534–1537.

[9] T. Du, A. Vijayakumar, K. B. Sundaram, and V. Desai, "Chemical mechanical polishing of nickel for applications in MEMS devices," *Microelectron. Eng.*, vol. 75, no. 2, pp. 234–241, Aug. 2004.

[10] M. Viviana, "Chromium in MEMS technology," *Mater. Sci. Res. J.*, vol. 5, pp. 1935–2441, Apr. 2011.

[11] M. Sohgawa *et al.*, "Tactile sensor array using microcantilever with nickel–chromium alloy thin film of low temperature coefficient of resistance and its application to slippage detection," *Sens. Actuators A, Phys.*, vol. 186, pp. 32–37, Oct. 2012.

[12] C. Xu and G. Piazza, "Artificial neural network based digital temperature compensation method for aluminum nitride MEMS resonators," in *Proc. IEEE Int. Ultrason. Symp. (IUS)*, Sep. 2017, pp. 1–4.

[13] M. Schneider, A. Bittner, and U. Schmid, "Thickness dependence of Young's modulus and residual stress of sputtered aluminum nitride thin films," *Appl. Phys. Lett.*, vol. 105, no. 20, Nov. 2014, Art. no. 201912.

[14] M. Schneider, M. Dorfmeister, P. Moll, M. Kaltenbacher, and U. Schmid, "Bi-stable aluminum nitride-based piezoelectric micromachined ultrasonic transducer (PMUT)," *J. Microelectromech. Syst.*, vol. 29, no. 5, pp. 948–953, Oct. 2020.

[15] M. Kucera *et al.*, "Characterization of a roof tile-shaped out-of-plane vibrational mode in aluminum-nitride-actuated self-sensing micro-resonators for liquid monitoring purposes," *Appl. Phys. Lett.*, vol. 104, no. 23, 2014, Art. no. 233501.

[16] M. Gillinger, T. Knobloch, M. Schneider, and U. Schmid, "Harsh environmental surface acoustic wave temperature sensor based on pure and scandium doped aluminum nitride on sapphire," *Proceedings*, vol. 1, no. 4, p. 341, 2017.

[17] E. Calayir, S. Merugu, J. Lee, N. Singh, and G. Piazza, "Heterogeneously integrated aluminum nitride MEMS resonators and filters," in *3D and Circuit Integration of MEMS*. Weinheim, Germany: Wiley-VCH GmbH, 2021, pp. 113–130.

[18] F. Patocka, M. Schlögl, C. Schneidhofer, N. Dörr, M. Schneider, and U. Schmid, "Piezoelectrically excited MEMS sensor with integrated planar coil for the detection of ferrous particles in liquids," *Sens. Actuators B, Chem.*, vol. 299, Nov. 2019, Art. no. 126957.

[19] M. G. Permenter, J. A. Lewis, and D. A. Jackson, "Exposure to nickel, chromium, or cadmium causes distinct changes in the gene expression patterns of a rat liver derived cell line," *PLoS ONE*, vol. 6, no. 11, Nov. 2011, Art. no. e27730.

[20] I. O. Igbokwe, E. Igwenagu, and N. A. Igbokwe, "Aluminium toxicosis: A review of toxic actions and effects," *Interdiscipl. Toxicol.*, vol. 12, no. 2, pp. 45–70, Oct. 2019.

[21] C. Coletti, M. J. Jaroszeski, A. Pallaoro, A. M. Hoff, S. Iannotta, and S. E. Saddow, "Biocompatibility and wettability of crystalline SiC and Si surfaces," in *Proc. 29th Annu. Int. Conf. IEEE Eng. Med. Biol. Soc.*, Aug. 2007, pp. 5849–5852.

[22] S. M. M. Dorfmeister and U. Schmid, "Static and dynamic performance of bistable MEMS membranes," *Sens. Actuators A, Phys.*, vol. 282, pp. 259–268, Oct. 2018.

[23] M. Dorfmeister, B. Kössl, M. Schneider, and U. Schmid, "A novel Bi-stable MEMS membrane concept based on a piezoelectric thin film actuator for integrated switching," *Proceedings*, vol. 2, no. 13, p. 912, 2019.

[24] P. Moll, G. Pfusterschmied, M. Schneide, M. Dorfmeister, and U. Schmid, "Piezoelectric switching of bistable MEMS membranes in fluids," in *Proc. IEEE 34th Int. Conf. Micro Electro Mech. Syst. (MEMS)*, Jan. 2021, pp. 544–547.

[25] T. Frischmuth *et al.*, "Low temperature deposition of a-SiC:H thin films applying a dual plasma source process," *Thin Solid Films*, vol. 616, pp. 164–171, Oct. 2016.

[26] X. Gao, X. Zhang, H. Tong, B. Lin, and J. Qin, "A simple elastic membrane-based microfluidic chip for the proliferation and differentiation of mesenchymal stem cells under tensile stress," *Electrophoresis*, vol. 32, no. 23, pp. 3431–3436, Dec. 2011.

[27] S. Toxiri, J. Ortiz, J. Masood, J. Fernández, L. A. Mateos, and D. G. Caldwell, "A wearable device for reducing spinal loads during lifting tasks: Biomechanics and design concepts," in *Proc. IEEE Int. Conf. Robot. Biomimetics (ROBIO)*, Dec. 2015, pp. 2295–2300.

[28] T. A. Desai, D. Hansford, and M. Ferrari, "Characterization of micromachined silicon membranes for immunoisolation and bioseparation applications," *J. Membr. Sci.*, vol. 159, no. 1, pp. 221–231, Jul. 1999.

[29] A. Nallathambi, T. Shanmuganantham, and D. Sindhanaiselvi, "Design and analysis of MEMS based piezoresistive pressure sensor for sensitivity enhancement," *Mater. Today, Proc.*, vol. 5, no. 1, pp. 1897–1903, 2018.

[30] M. Narducci, L. Yu-Chia, W. Fang, and J. Tsai, "CMOS MEMS capacitive absolute pressure sensor," *J. Micromech. Microeng.*, vol. 23, no. 5, 2013, Art. no. 055007.

[31] X. Wang, B. Li, O. L. Russo, H. T. Roman, K. K. Chin, and K. R. Farmer, "Diaphragm design guidelines and an optical pressure sensor based on MEMS technique," *Microelectron. J.*, vol. 37, no. 1, pp. 50–56, Jan. 2006.

[32] R. A. M. Receveur, C. R. Marxer, R. Woering, V. C. M. H. Larik, and N.-F. de Rooij, "Laterally moving bistable MEMS DC switch for biomedical applications," *J. Microelectromech. Syst.*, vol. 14, no. 5, pp. 1089–1098, 2005.

[33] B. Wagner, H. J. Quenzer, S. Hoerschelmann, T. Lisec, and M. Juerss, "Bistable microvalve with pneumatically coupled membranes," in *Proc. 9th Int. Workshop Micro Electromech. Syst.*, Feb. 1996, pp. 384–388.

[34] K. Yamashita, H. Hibino, T. Nishioka, M. Noda, and P. Muralt, "Vibration mode of MEMS ultrasonic sensors on buckled diaphragms with piezoelectric resonance frequency modification," in *Proc. IEEE Sensors*, Oct. 2019, pp. 1–4.

[35] W. K. Schomburg and C. Goll, "Design optimization of bistable microdiaphragm valves," *Sens. Actuators A, Phys.*, vol. 64, pp. 259–264, Jan. 1998.

[36] V. Ahola, L. Soederlund, M. Linjama, M. Juhola, and L. Kettune, "Novel bistable hammer valve for digital hydraulics," *Int. J. Fluid Power*, vol. 11, no. 3, p. 35–44, Jan. 2010.

[37] X. Miao, X. Dai, P. Wang, G. Ding, and X. Zhao, "Design, fabrication and characterization of a bistable electromagnetic microrelay with large displacement," *Microelectron. J.*, vol. 42, pp. 992–998, Aug. 2011.

[38] M. Dorfmeister, B. Kössl, M. Schneider, G. Pfusterschmied, and U. Schmid, "Switching performance of bistable membranes activated with integrated piezoelectric thin film transducers," *J. Micromech. Microeng.*, vol. 29, no. 10, 2019, Art. no. 105008.

[39] M. Dorfmeister, M. Schneider, and U. Schmid, "3D characterisation of piezoelectric bistable MEMS membranes during switching," *Sens. Actuators A, Phys.*, vol. 298, Oct. 2019, Art. no. 111576.

[40] R. I. Freshney, "Culture of specific cell types," in *Culture of Animal Cells*. Weinheim, Germany: Wiley-VCH GmbH, 2005.

[41] A. Angelescu *et al.*, "Porous silicon matrix for applications in biology," *Rev. Adv. Mater. Sci.*, vol. 5, no. 5, pp. 440–449, Dec. 2003.

[42] A. Pizzoferrato *et al.*, "Cell culture methods for testing biocompatibility," *Clin. Mater.*, vol. 15, no. 3, pp. 173–190, Jan. 1994.

[43] J. Rach, B. Halter, and M. Aufderheide, "Importance of material evaluation prior to the construction of devices for *in vitro* techniques," *Experim. Toxicolog. Pathol.*, vol. 65, nos. 7–8, pp. 973–978, Nov. 2013.

[44] M. Catauro, F. Bollino, F. Papale, M. Gallicchio, and S. Pacifico, "Influence of the polymer amount on bioactivity and biocompatibility of SiO_2/PEG hybrid materials synthesized by sol–gel technique," *Mater. Sci. Eng., C*, vol. 48, pp. 548–555, Mar. 2015.

[45] J. Fogh, W. C. Wright, and J. D. Loveless, "Absence of HeLa cell contamination in 169 cell lines derived from human tumors," *J. Nat. Cancer Inst.*, vol. 58, no. 2, pp. 209–214, Feb. 1977.

[46] Y. Sambuy, I. De Angelis, G. Ranaldi, M. L. Scarino, A. Stammati, and F. Zucco, "The Caco-2 cell line as a model of the intestinal barrier: Influence of cell and culture-related factors on Caco-2 cell functional characteristics," *Cell Biol. Toxicol.*, vol. 21, no. 1, pp. 1–26, Jan. 2005.

[47] T. Lea, "Caco-2 cell line," in *The Impact of Food Bioactives on Health: In Vitro and Ex Vivo Models*, K. Verhoeckx *et al.*, Eds. Cham, Switzerland: Springer, 2015, pp. 103–111.

[48] S. Jalili-Firoozinezhad *et al.*, "A complex human gut microbiome cultured in an anaerobic intestine-on-a-chip," *Nature Biomed. Eng.*, vol. 3, no. 7, pp. 520–531, Jul. 2019.

[49] S. Lama, O. Merlin-Zhang, and C. Yang, "*In vitro* and *in vivo* models for evaluating the oral toxicity of nanomedicines," *Nanomaterials*, vol. 10, no. 11, p. 2177, Oct. 2020.

[50] B. Srinivasan, A. R. Kolli, M. B. Esch, H. E. Abaci, M. L. Shuler, and J. J. Hickman, "TEER measurement techniques for *in vitro* barrier model systems," *J. Lab. Autom.*, vol. 20, no. 2, pp. 107–126, Apr. 2015.

[51] I. S. Sohal, K. S. O'Fallon, P. Gaines, P. Demokritou, and D. Bello, "Ingested engineered nanomaterials: State of science in nanotoxicity testing and future research needs," *Part. Fibre Toxicol.*, vol. 15, no. 1, pp. 1–31, Dec. 2018.

[52] X. Liu *et al.*, "Ingestible hydrogel device," *Nature Commun.*, vol. 10, no. 1, p. 493, Dec. 2019.

[53] I. Guell *et al.*, "Influence of structured wafer surfaces on the characteristics of Caco-2 cells," *Acta Biomaterialia*, vol. 5, no. 1, pp. 288–297, Jan. 2009.

[54] T. J. Kinnari *et al.*, "Adhesion of staphylococcal and Caco-2 cells on diamond-like carbon polymer hybrid coating," *J. Biomed. Mater. Res. A*, vol. 86A, no. 3, pp. 760–768, Sep. 2008.

[55] L. Wang, B. Sun, K. S. Ziemer, G. A. Barabino, and R. L. Carrier, "Chemical and physical modifications to poly(dimethylsiloxane) surfaces affect adhesion of Caco-2 cells," *J. Biomed. Mater. Res. A, Off. J. Soc. Biomater., Jpn. Soc. Biomater., Austral. Soc. Biomater. Korean Soc. Biomater.*, vol. 93, no. 4, pp. 1260–1271, Jun. 15, 2010.

[56] M. J. Briske-Anderson, J. W. Finley, and S. M. Newman, "The influence of culture time and passage number on the morphological and physiological development of Caco-2 cells," *Experim. Biol. Med.*, vol. 214, no. 3, pp. 248–257, Mar. 1997.

[57] G. Kim *et al.*, "The biocompatability of mesoporous inorganic–organic hybrid resin films with ionic and hydrophilic characteristics," *Biomaterials*, vol. 31, no. 9, pp. 2517–2525, Mar. 2010.

[58] S. Al-Nasiry, N. Geusens, M. Hanssens, C. Luyten, and R. Pijnenborg, "The use of Alamar Blue assay for quantitative analysis of viability, migration and invasion of choriocarcinoma cells," *Hum. Reprod.*, vol. 22, no. 5, pp. 1304–1309, May 2007.

[59] E. Bogner *et al.*, "Bridging the gap—Biocompatibility of microelectronic materials," *Acta Biomaterialia*, vol. 2, no. 2, pp. 229–237, Mar. 2006.

[60] M. D. Persidsky and G. S. Baillie, "Fluorometric test of cell membrane integrity," *Cryobiology*, vol. 14, no. 3, pp. 322–331, Jun. 1977.

[61] K. V. Christ and K. T. Turner, "Methods to measure the strength of cell adhesion to substrates," *J. Adhes. Sci. Technol.*, vol. 24, nos. 13–14, pp. 2027–2058, Jan. 2010.

[62] A. Khalili and M. Ahmad, "A review of cell adhesion studies for biomedical and biological applications," *Int. J. Mol. Sci.*, vol. 16, no. 8, pp. 18149–18184, Aug. 2015.

[63] L. S. L. Cheung *et al.*, "Detachment of captured cancer cells under flow acceleration in a bio-functionalized microchannel," *Lab Chip*, vol. 9, no. 12, pp. 1721–1731, 2009.

[64] S. Shiri, K. F. Martin, and J. C. Bird, "Surface coatings including fingerprint residues can significantly alter the size and shape of bloodstains," *Forensic Sci. Int.*, vol. 295, pp. 189–198, Feb. 2019.

[65] C. Poon, "Measuring the density and viscosity of culture media for optimized computational fluid dynamics analysis of *in vitro* devices," *bioRxiv*, vol. 126, Jan. 2020, Art. no. 266221.